ARTICLE NO. 79-0760R

Effect of Load Sequence on the Statistical Fatigue of Composites

J. N. Yang* and D. L. Jones†
The George Washington University, Washington, D.C.

A residual strength degradation model has been applied to predict the effect of loading sequence on the statistical distributions of the fatigue life and the residual strength under n stress levels of cyclic loading. In particular, the dual stress fatigue cumulative damage is studied in detail and Miner's sum (the cumulative damage sum at fatigue failure) is shown to be a statistical variable. It is shown theoretically that Miner's sum is greater than or equal to unity for the high-low load sequence, while it is smaller than or equal to unity for the low-high load sequence, with the deviation from unity increasing as the difference between the high and the low stress levels increases. An experimental test program using graphite/epoxy $[\pm 45^\circ]_{2s}$ angle-ply laminates has been carried out to generate statistically meaningful data for verifying the proposed approach. It is shown that the correlation between the test results and the theoretical predictions of the fatigue life distribution for graphite/epoxy $[\pm 45^\circ]_{2s}$ angle-ply laminates is reasonable.

Introduction

SINCE composite materials possess mechanical properties, such as low weight, high strength, high stiffness, etc., that are superior to conventional metallic materials, considerable emphasis has been placed on the application of advanced composite materials to aircraft structures. One of the most important problems in the design of aircraft structures is to account for the effect of fatigue loading. It is well-known that the dispersion of the fatigue life of composites is very large. The problem is further complicated by the fact that service loadings on aircraft structures are random in nature, although the analysis is often simplified by the use of spectrum loadings. As a result, a statistical approach is essential to the fatigue analysis of composite materials.

Unfortunately, most of the research efforts in the fatigue behavior of composites,[1-12] with two exceptions,[13-14] have not investigated the effect of load sequence. Broutman and Sahu[13] conducted fatigue tests on glass/epoxy coupon specimens, and concluded that the residual strength of glass/epoxy laminates degrades linearly with respect to the number of load cycles. They also proposed a theory for the effect of loading sequence on the fatigue behavior based upon this premise. However, extensive investigations of the fatigue behavior of advanced composite materials, such as graphite/epoxy, boron/epoxy, etc., indicate that the residual strength decreases according to a highly nonlinear function of the number of fatigue cycles.[1-11] In addition, some recent considerations of load sequence effects have been reported.[14]

It has been observed[5,9-11,15] that the stiffness of composite materials decays under fatigue loadings. Investigation of the stiffness degradation under fatigue loading is of practical importance in application, since the detection of the residual stiffness in service is nondestructive. If the stiffness degradation can be related to the degradation of the residual strength and hence the fatigue life, then the fatigue damage or the fatigue life can be predicted nondestructively by measurement of the residual stiffness.[15] Preliminary test results have been obtained and presented.

Presented as Paper 79-0760 at the AIAA/ASME/ASCE/AHS 20th Structures, Structural Dynamics and Materials Conference, St. Louis, Mo., April 4-6, 1979; submitted Oct. 5, 1979; revision received April 16, 1980.

Index categories: Structural Composite Materials; Structural Durability (including Fatigue and Fracture); Materials, Properties of.

*Professor, School of Engineering and Applied Science. Member AIAA.

†Associate Professor, School of Engineering and Applied Science.

Load Sequence Effect

The residual strength degradation model discussed in this section has been in existence for some time. Therefore, the development of the model will not be presented in this section, but emphasis will be placed on generalizing the model to include load sequence effects due to a sequence of two fatigue loadings and to spectrum loadings. A residual strength degradation model for unnotched composite laminates under cyclic loading can be written as,[3-5]

$$R^c(n_1) = R^c(n_0) - \beta^c K S^b (n_1 - n_0) \tag{1}$$

in which $R(n_1)$ and $R(n_0)$ are the residual strengths at n_1 and n_0 cycles ($n_1 > n_0$), respectively; β is the scale parameter of the ultimate strength; b, c, and K are three parameters to be determined from the test data; S is the stress range defined as $S = \sigma_{max} - \sigma_{min} = (1-R)\sigma_{max}$, where σ_{max} and σ_{min} represent the maximum and the minimum cyclic stresses, respectively; and R is the stress ratio.

Equation (1) indicates that the residual strength $R(n_1)$ at n_1 cycles can be expressed in terms of the residual strength $R(n_0)$ at the previous load cycles n_0, the stress range S, and the number of load cycles from n_0 to n_1, i.e., $n_1 - n_0$.

For $n_0 = 0$ and $n_1 = n$, Eq. (1) reduces to

$$R^c(n) = R^c(0) - \beta^c K S^b n \tag{2}$$

where $R(0)$ is the ultimate strength.

The ultimate strength is a statistical variable assumed to follow the two parameter Weibull distribution,

$$F_{R(0)}(x) = P[R(0) \le x] = 1 - \exp[-(x/\beta)^\alpha] \tag{3}$$

where $F_{R(0)}(x)$ is the probability that the ultimate strength is smaller than a value x, α is the shape parameter, and β is the scale parameter (or the characteristic strength). Both α and β should be determined from the test results of the ultimate strength.

Sequence of Two Fatigue Loadings

Because of the relative simplicity in explaining the effect of loading sequence on the fatigue behavior of composites, the theoretical derivation and the physical interpretation for two

load levels are presented first. The general solution for the n loading sequence or for spectrum loading will be derived later.

The theoretical model represented by Eq. (1) can be used to predict the effect of the loading sequence on the statistical distributions of the fatigue life and the residual strength. Let the specimen be subjected to a sequence of two fatigue loadings, with constant stress ratio and maximum stresses $\sigma_{1\max}$ and $\sigma_{2\max}$, respectively, for n_1 and n_2 cycles as shown in Fig. 1. From Eq. (2) the residual strength after the application of the first fatigue loading $R(n_1)$ can be expressed in terms of $R(0)$ as

$$R^c(n_1) = R^c(0) - \beta^c K S_1^b n_1 \tag{4}$$

After the second fatigue loading has been applied, the residual strength $R(n_1+n_2)$ at n_1+n_2 cycles can be expressed in terms of $R(n_1)$ as,

$$R^c(n_1+n_2) = R^c(n_1) - \beta^c K S_2^b n_2 \tag{5}$$

Summation of Eqs. (4) and (5) leads to the expression for the residual strength $R(n_1+n_2)$, as follows,

$$R^c(n_1+n_2) = R^c(0) - \beta^c K(S_1^b n_1 + S_2^b n_2) \tag{6}$$

The statistical distribution of the residual strength after n_1+n_2 load cycles can be obtained from Eq. (6) as follows,

$$F_{R(n_1+n_2)}(x) = P[R(n_1+n_2) \le x]$$
$$= P[R(0) \le \{x^c + \beta^c K(S_1^b n_1 + S_2^b n_2)\}^{1/c}] \tag{7}$$

Substitution of Eq. (3) into Eq. (7) yields the distribution function of the residual strength as,

$$F_{R(n_1+n_2)}(x) = 1 - \exp\left\{-\left[\frac{x^c + \beta^c K(S_1^b n_1 + S_2^b n_2)}{\beta^c}\right]^{\alpha/c}\right\},$$
$$x \ge \sigma_{2\max} \tag{8}$$

Equation (8) is a three-parameter Weibull distribution with a negative lower bound at $-\beta^c K(S_1^b n_1 + S_2^b n_2)$. The negative lower bound comes from the possibility that the residual strength may be reduced below zero after n_1+n_2 cycles. Since fatigue failure occurs when the residual strength decays to a value below the maximum applied stress $\sigma_{2\max}$, the distribution function holds for $x \ge \sigma_{2\max}$ as indicated. With characteristic lives defined as,

$$\tilde{N}_1 = 1/KS_1^b, \quad \tilde{N}_2 = 1/KS_2^b \tag{9}$$

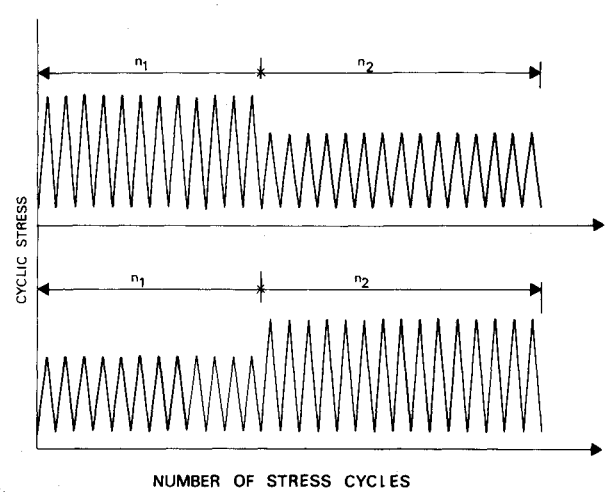

Fig. 1 Typical high-low and low-high load sequences.

Eq. (8) can be written as follows

$$F_{R(n_1+n_2)}(x) = 1 - \exp\left\{-\left[\left(\frac{x}{\beta}\right)^c + \frac{n_1}{\tilde{N}_1} + \frac{n_2}{\tilde{N}_2}\right]^{\alpha/c}\right\},$$
$$x \ge \sigma_{2\max} \tag{10}$$

If the number of load cycles under the second fatigue loading is increased until fracture, then the fatigue life N_{12}, denoting the number of load cycles to failure under the second fatigue loading, is a statistical variable. Hence, the fatigue failure occurs when

$$R(n_1+n_2) = \sigma_{2\max}, \quad N_{12} = n_2 \tag{11}$$

Substitution of Eq. (11) into Eq. (6) leads to the following expression for the fatigue life,

$$N_{12} = [R^c(0) - \sigma_{2\max}^c - \beta^c K S_1^b n_1]/\beta^c K S_2^b \tag{12}$$

The distribution function of the fatigue life under the second fatigue loading can be obtained through the transformation of Eq. (12) as follows,

$$F_{N_{12}}(n) = 1 - \exp\left\{-\left[\frac{n}{\tilde{N}_2} + \frac{n_1}{\tilde{N}_1} + \left(\frac{\sigma_{2\max}}{\beta}\right)^c\right]^{\alpha/c}\right\} \tag{13}$$

It is observed from Eq. (13) that the distribution function of the fatigue life is a three-parameter Weibull distribution with a negative lower bound at $-[n_1(\tilde{N}_2/\tilde{N}_1) + \tilde{N}_2(\sigma_{2\max}/\beta)^c]$. The first term in the bracket represents the possibility that the specimen may fail under the first fatigue loading and the second term is contributed by the possibility that the specimen may fail instantaneously upon the application of the second fatigue loading.

The probability of failure under the first fatigue loading, denoted by p_1, can be obtained from Eq. (13) by setting $n=0$ and replacing $\sigma_{2\max}$ by $\sigma_{1\max}$ as follows,

$$p_1 = 1 - \exp\left\{-\left[\frac{n_1}{\tilde{N}_1} + \left(\frac{\sigma_{1\max}}{\beta}\right)^c\right]^{\alpha/c}\right\} \tag{14}$$

Let N_{12}^* be the fatigue life under the second fatigue loading for those specimens which have survived n_1 cycles of the first fatigue loading, i.e, $N_{12}^* \ge 0$. Then, the statistical distribution of N_{12}^* can be derived as,

$$F_{N_{12}^*}(n) = P[N_{12}^* \le n] = 1 - \{P[N_{12} > n]/P[N_{12} > 0]\} \tag{15}$$

Substitution of Eqs. (13) and (14) into Eq. (15) leads to

$$F_{N_{12}^*}(n) = 1 - (1-p_1)^{-1}\exp\left\{-\left[\frac{n}{\tilde{N}_2} + \frac{n_1}{\tilde{N}_1} + \left(\frac{\sigma_{2\max}}{\beta}\right)^c\right]^{\alpha/c}\right\} \tag{16}$$

in which p_1 is given by Eq. (14).

It is observed from Eq. (6) that $R(n_1+n_2)$ is independent of the load sequence and hence so is its statistical distribution given by Eq. (10). Moreover, the fatigue life N_{12} given by Eq. (12) and its statistical distributions represented by Eqs. (13) and (16) do depend weakly on the sequence of cyclic loading. The weak dependence comes from the term associated with $\sigma_{2\max}$ which is usually small in comparison with the other terms.

Graphical Interpretation

Since the residual strength, the fatigue life, and their statistical distributions have been derived for specimens subjected to a sequence of two distinct fatigue loadings, a graphical interpretation of the model will be made to explain

its underlying physical meaning. Moreover, it will be demonstrated through the graphical interpretation that Miner's sum does indeed depend on the loading sequence.

The model given by Eq. (2) is a stochastic equation, since both $R(n)$ and $R(0)$ are statistical variables. If $R_\gamma(0)$ denotes the γth percentile of the ultimate strength, i.e., the probability that the ultimate strength is smaller than or equal to the value $R_\gamma(0)$ is,

$$\gamma(\%) = P[R(0) \le R_\gamma(0)] = F_{R(0)}[R_\gamma(0)] \tag{17}$$

Then, Eq. (2) can be written as,

$$R_\gamma^c(n) = R_\gamma^c(0) - \beta^c K S^b n \tag{18}$$

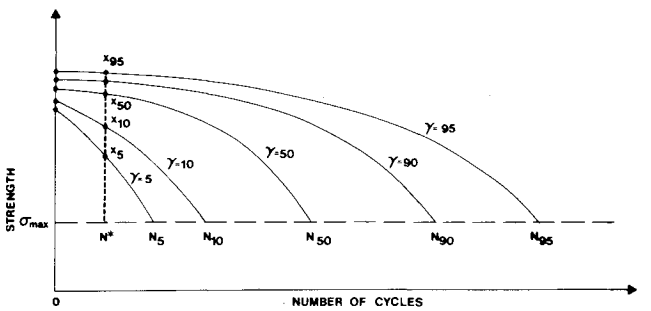

Fig. 2 Residual strength-fatigue life-probability diagram.

in which $R_\gamma(n)$ is the γth percentile of the residual strength $R(n)$. By varying the value of γ, for instance $\gamma = 5, 10, 50, 90, 95\%$, a family of curves of the corresponding percentiles can be constructed from Eq. (18) for a specific value of σ_{max} as shown schematically in Fig. 2. The family of curves of percentiles of the residual strength is called the equal probability curve. The statistical distribution of the fatigue life is also provided by the family of percentiles N_γ that denotes the number of cycles at which γ percent of a set of specimens have failed. As a result, Fig. 2 represents a residual strength-fatigue life-probability diagram.

It is obvious that Eq. (18) and hence Fig. 2 depend on σ_{max} (or the stress range S); the larger σ_{max} (or S) is, the faster the strength degradation will occur. Hence, Eq. (18) represents an infinite set of curves corresponding to an infinite number of maximum stress levels.

Finally, corresponding to a particular percentile γ (or probability) but with different maximum stress levels, the $R(n) - \sigma_{max} - N$ diagram can be drawn from Eq. (18); for instance, $\gamma = 50\%$ as shown in Fig. 3. In Fig. 3, the $R_{50}(n)$ curves are the median residual strength curves (solid curves), while the N_{50} curve is the median fatigue life (dash-dot curve), indicating the 50% reliability fatigue lives.

A sample specimen corresponds to a particular sample percentile, i.e., the γth percentile. When it is subjected to a cyclic loading at the maximum stress σ_{1max}, its γth percentile residual strength follows curve A as shown in Fig. 4a. Instead, if the same specimen is subjected to a cyclic loading with the maximum stress σ_{2max} ($\sigma_{1max} > \sigma_{2max}$), then the residual strength will follow curve B of Fig. 4a. Both curves start from

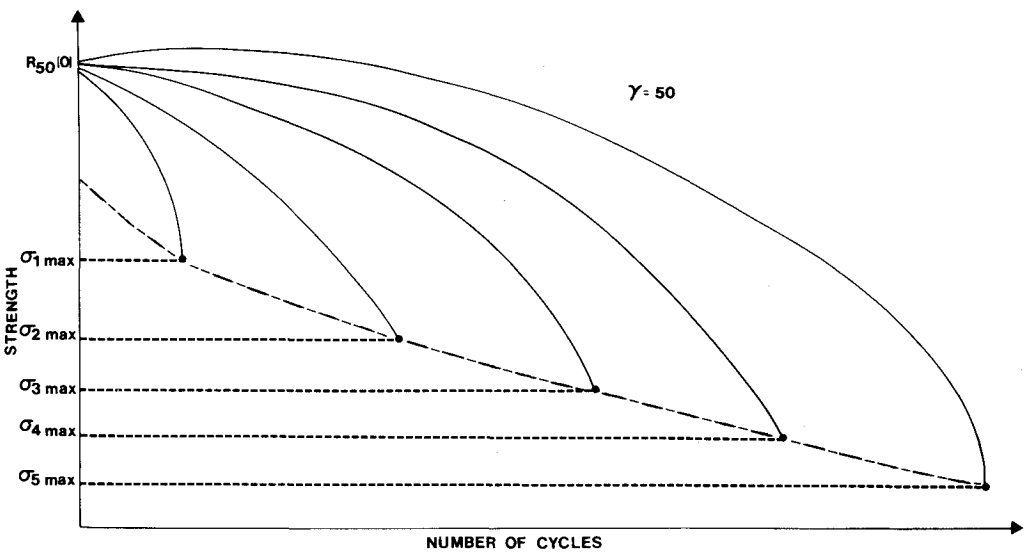

Fig. 3 Residual strength-maximum cyclic stress-fatigue life ($R(n) - \sigma_{max} - N$) diagram for $\gamma = 50$.

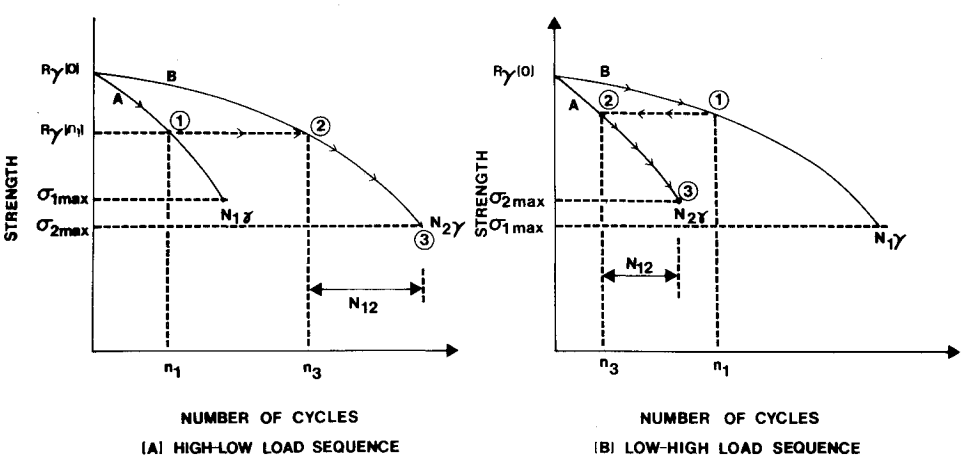

Fig. 4 Residual strength degradation under high-low and low-high load sequences.

the same ultimate strength $R_\gamma(0)$ but end at different fatigue lives $N_{1\gamma}$ and $N_{2\gamma}$. The effect of loading sequence will be further explained using Fig. 4.

High-Low Loading Sequence, $\sigma_{1\max} > \sigma_{2\max}$

If $\sigma_{1\max}$ is applied to the specimen for n_1 cycles and then followed by $\sigma_{2\max}$ until fracture (with probability of $\gamma\%$), then the residual strength after the application of the high load is computed from Eq. (18) in which $n=n_1$ and $S=S_1$. $R_\gamma(n_1)$ can also be obtained graphically at point ① following curve A [starting from $R_\gamma(0)$] as shown in Fig. 4a. It is then moved horizontally from point ① to point ② on curve B which corresponds to n_3 cycles. This indicates that the same residual strength would have been obtained if the specimen were subjected to $\sigma_{2\max}$ for n_3 cycles. Upon the application of the low load, the residual strength starts to decay from point ② following curve B until the specimen fractures at point ③ as shown in Fig. 4a. The number of cycles to failure under the low load is $N_{2\gamma}-n_3$ (see Fig. 4a). The total number of load cycles to failure under both loadings is $n_1+N_{2\gamma}-n_3$.

Low-High Loading Sequence, $\sigma_{1\max} < \sigma_{2\max}$

If $\sigma_{1\max}$ is applied to the same specimen for n_1 cycles and then followed by $\sigma_{2\max}$ until fracture, the residual strength degradation path is given by $R_\gamma(0) \rightarrow ① \rightarrow ② \rightarrow ③$ as shown in Fig. 4b. The number of cycles to failure under the high load is $N_{2\gamma}-n_3$ (see Fig. 4b). The total number of load cycles to failure under both loadings is $n_1+N_{2\gamma}-n_3$ (see Fig. 4b).

Probabilistic Interpretation of Miner's Damage Sum

Let N_1 and N_2 be the fatigue lives of composite specimens under the fatigue loadings $\sigma_{1\max}$ (with stress range S_1) and $\sigma_{2\max}$ (with stress range S_2), respectively, in which $\sigma_{1\max}$ may be greater or smaller than $\sigma_{2\max}$. If the specimen is first subjected to $\sigma_{1\max}$ for n_1 cycles followed by the fatigue loading $\sigma_{2\max}$ until fracture, then the number of cycles to failure under $\sigma_{2\max}$ is denoted by N_{12}. The Miner's damage sum at fatigue failure, denoted by D, is therefore,

$$D=\frac{n_1}{N_1}+\frac{N_{12}}{N_2} \tag{19}$$

It follows from Eq. (19) that the damage sum D at fatigue failure is a statistical (random) variable, since the fatigue lives N_1, N_2, and N_{12} are statistical variables. The fatigue lives N_1 and N_2 can be obtained by substituting the conditions for fatigue failure i.e., $n=N_1$, $R(n)=\sigma_{1\max}$ or $n=N_2$, $R(n)=\sigma_{2\max}$, into Eq. (2), yielding

$$N_1=[R^c(0)-\sigma_{1\max}^c]/\beta^c K S_1^b \tag{20}$$

$$N_2=[R^c(0)-\sigma_{2\max}^c]/\beta^c K S_2^b \tag{21}$$

The fatigue life N_{12} under the second fatigue loading is given by Eq. (12). Substitution of Eqs. (12, 20, and 21) into Eq. (19) leads to an expression for Miner's sum in the form;

$$D=1+\frac{n_1\beta^c}{\tilde{N}_1}\left[\frac{1}{R^c(0)-\sigma_{1\max}^c}-\frac{1}{R^c(0)-\sigma_{2\max}^c}\right] \tag{22}$$

in which $\tilde{N}_1=1/KS_1^b$ is given by Eq. (9).

The following observations can be plausibly obtained from Eq. (22):

1) Under the high-low loading sequence, where $\sigma_{1\max}>\sigma_{2\max}$, Miner's sum is always greater than unity and the lower bound of D is unity when $\sigma_{1\max}=\sigma_{2\max}$, i.e, $D\geq 1$. Furthermore, D increases as the difference between $\sigma_{1\max}$ and $\sigma_{2\max}$ increases.

2) Under the low-high loading sequence, where $\sigma_{1\max}<\sigma_{2\max}$, Miner's sum is always smaller than unity and the upper bound of D is unity when $\sigma_{1\max}=\sigma_{2\max}$, i.e., $D\leq 1$. Furthermore, D decreases as the difference between $\sigma_{1\max}$ and $\sigma_{2\max}$ increases.

3) The deviation of Miner's sum from unity increases as the damage accumulated under the first fatigue loading increases, i.e., as $n_1/\tilde{N}_1$ increases.

From the observations made above, the low-high load sequence is more damaging. The probability density function of the Miner's sum D is schematically displayed in Fig. 5 for the low-high and the high-low load sequences.

Statistical Fatigue under Spectrum Loading

Let a specimen be subjected to a spectrum loading in which the maximum stress of each load cycle is denoted by $\sigma_{1\max}$, $\sigma_{2\max},\ldots,\sigma_{j\max}$. The sequence of stress ranges for the spectrum loading is denoted by $S_1, S_2,\ldots,S_j$.

According to the residual strength degradation model given in Eq. (1), the residual strength can be expressed cycle by cycle as follows:

$$\left.\begin{aligned} R^c(1)&=R^c(0)-\beta^c K S_1^b \\ R^c(2)&=R^c(1)-\beta^c K S_2^b \\ &\cdots\cdots \\ R^c(n)&=R^c(n-1)-\beta^c K S_n^b \end{aligned}\right\} \tag{23}$$

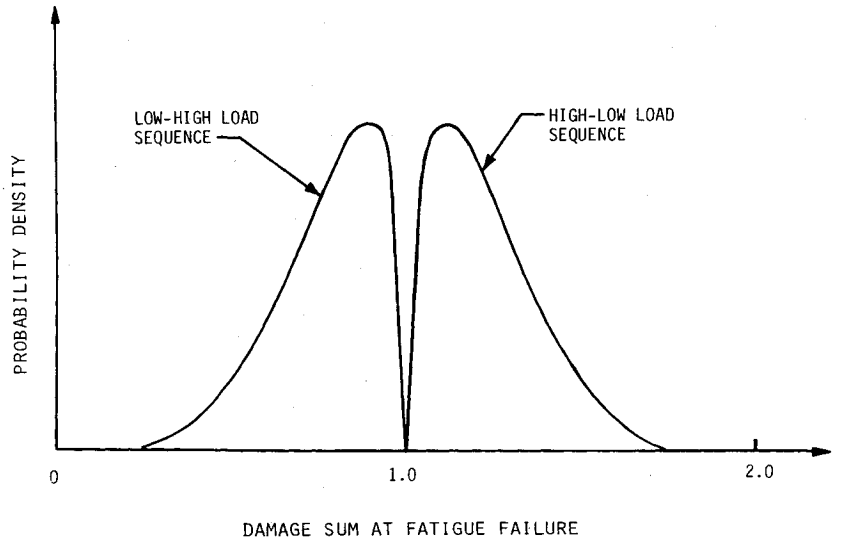

Fig. 5 Illustration of probability density function of damage sum for low-high and high-low load sequences.

Summation of Eq. (23) yields the residual strength $R(n)$ after n load cycles in terms of the ultimate strength $R(0)$ as,

$$R^c(n) = R^c(0) - \beta^c K \sum_{i=1}^{n} S_i^b \tag{24}$$

It should be noticed that for generality, the maximum stress for each load cycle is considered different. Under spectrum loadings, some of the load cycles will have the same maximum stress and hence represent a special case.

The statistical distribution of the residual strength $R(n)$ after n cycles of spectrum loading can be derived from that of the ultimate strength $R(0)$, given by Eq. (3), through the transformation of Eq. (24) as follows,

$$F_{R(n)}(x) = 1 - \exp\left\{-\left[\left(\frac{x}{\beta}\right)^c + \sum_{i=1}^{n} \frac{1}{\tilde{N}_i}\right]^{\alpha/c}\right\}, \quad x \geq \sigma_{n\max} \tag{25}$$

in which

$$\tilde{N}_i = 1/KS_i^b \quad \text{for } i = 1,2,\ldots,n \tag{26}$$

Let N be the fatigue life of the specimen under spectrum loading. Then, a fatigue failure occurs at the nth fatigue cycle when the residual strength, $R(n-1)$, is smaller than the applied stress, $\sigma_{n\max}$. Hence, the probability of a fatigue failure at the nth fatigue load cycle is given by p_n

$$p_n = P[R(n-1) \leq \sigma_{n\max}]$$

$$= 1 - \exp\left\{-\left[\left(\frac{\sigma_{n\max}}{\beta}\right)^c + \sum_{i=1}^{n-1} \frac{1}{\tilde{N}_i}\right]^{\alpha/c}\right\} \tag{27}$$

in which Eqs. (24) and (25) have been used.

It can be observed from Eq. (25) that the statistical distributions of the residual strength does not depend on the load sequence before the nth load cycles.

Test Results and Experimental Verification

A test program using coupon specimens of 5208/T300 graphite/epoxy $[\pm 45^\circ]_{2s}$ laminates was initiated for the purpose of generating statistically significant test data to evaluate the validity of the theoretical approach described. The specimen dimensions were nominally $38.1 \times 1.01 \times 254$ mm ($1.5 \times 0.04 \times 10$ in.). For uniaxial loading of these specimens, it has been shown that the shear stress is equal to one-half of the axial stress.[17,18]

Fifteen tests were performed to determine the ultimate shear strength and to establish values for the two parameters α and β in the Weibull distribution [Eq. (3)]. The tests were performed at a rate that would approximate failure during the first load excursion of the fatigue test program. The two-parameter Weibull distribution given by Eq. (3) were used to fit the test data, yielding

$$\alpha = 43.073, \quad \beta = 99.63 \text{ MPa } (14.45 \text{ ksi}) \tag{28}$$

A set of 33 fatigue scan tests under different maximum cyclic stresses have also been conducted. For all of these tests, the loading frequency was 10 Hz and the stress ratio was 0.1. The fatigue scan data consisting of 27 fatigue failure tests and 6 residual strength tests were given in Ref. 5. The fatigue scan data and the ultimate shear strength data were used to determine the values of b, c, and K appearing in the fatigue and residual strength degradation model with the results[5]

$$c = 10.0, \quad b = 15.68, \quad K = 4.73 \times 10^{-32} (6.65 \times 10^{-19}) \tag{29}$$

in which the unit of the strengths $R(0)$ and $R(n)$ and the applied stress range S is MPa (ksi). After the values of α, β, b, c, and K are determined, the model described can then predict the statistical distributions of the fatigue life and the residual strength under high-low or low-high load sequences without the need for further experimental data.

To verify the accuracy of the theoretical approach in predicting the statistical distributions of the fatigue life under a sequence of fatigue loadings, 17 specimens were tested under a low-high fatigue loading sequence. The specimens were subjected to the first fatigue loading with a maximum shear stress, $\sigma_{1\max} = 51.7$ MPa (7.5 ksi), and a stress range, $S_1 = 46.5$ MPa (6.75 ksi) for $n_1 = 73{,}930$ cycles. Then, the specimens were further subjected to the second fatigue loading with a maximum shear stress $\sigma_{2\max} = 60.7$ MPa (8.8 ksi) and a stress range $S_2 = 54.6$ MPa (7.92 ksi) until fracture occurred. The test results are presented in Table 1.

According to the theoretical prediction given by Eq. (14), the probability that the specimen will fail under the first fatigue loading (low load) is 5%. Hence, the average number of specimens expected to fail under the low load is $0.05 \times 17 = 0.85$. The test results shown in Table 1 indicate no failures. However, the fatigue life of the first specimen which survived only 140 cycles under the second fatigue loading is extremely short and it does not belong to the same population as the rest of the data (see Fig. 1). Therefore, it is reasonable to consider it as a failure under the first fatigue loading.

The results of the fatigue life under the high load for those specimens which survived the low load are plotted in Fig. 6 as open circles. Also plotted in Fig. 6 as a solid curve is the theoretical prediction obtained from Eq. (16). It can be observed from Fig. 6 that the correlation between the theoretical prediction and the test data on the statistical distribution of the fatigue life under the high load is excellent.

The median value of the ultimate shear strength follows from Eq. (3) as $R_{50}(0) = \beta[-\ln(1-0.5)]^{1/\alpha} = 98.788$ MPa (14.328 ksi). The characteristic fatigue lives under the low and the high loads alone, respectively, can be computed from Eq. (9) as $\tilde{N}_1 = 149{,}200$ cycles, $\tilde{N}_2 = 12{,}170$ cycles. The median values of the fatigue lives, N_1 and N_2, under the low and high loads alone, respectively, are computed using Eqs. (20) and (21) with $R(0)$ being replaced by $R_{50}(0)$ as follows: $\hat{N}_1 = [R_{50}^c(0) - \sigma_{1\max}^c]/\beta^c K S_1^b = 136{,}860$ cycles, and $\hat{N}_2 = [R_{50}^c(0) - \sigma_{2\max}^c]/\beta^c K S_2^b = 11{,}095$ cycles.

From the information given above, the median value of the Miner's sum based upon the theoretical model D_{50} is computed from Eq. (22), with $n_1 = 73{,}940$ and $R(0)$ being replaced by $R_{50}(0)$, as $D_{50} = 0.9967$.

The median data, i.e., the 50% data point, in Table 1 is 4810 cycles (the ninth data point). Hence, the median value of

Table 1 Fatigue life and residual stiffness under low-high load sequence, $\sigma_{1\max} = 51.7$ MPa (7.5 ksi), $\sigma_{2\max} = 60.7$ MPa (8.8 ksi), $n_1 = 73{,}940$ cycles

Specimen No.	Fatigue life under high load, cycles	Initial stiffness, MPa (ksi)	Residual stiffness, MPa (ksi)[a]
A2-6	140	5619(815)	5068(735)
A1-17	1,200	5516(800)	5171(750)
A3-15	1,740	5619(815)	5343(775)
A2-14	3,300	5550(805)	5264(762)
A2-43	3,350	5378(780)	5102(740)
A1-53	3,740	5516(800)	5171(750)
A3-26	4,710	5861(850)	5516(800)
A3-34	4,730	5895(855)	5343(775)
A2-49	4,810	5792(840)	5343(775)
A1-51	5,280	5343(775)	5102(740)
A3-56	5,340	5929(860)	5343(775)
A1-56	5,470	5412(785)	4999(725)
A1-40	5,610	5516(800)	5171(750)
A3-31	5,820	5516(800)	5102(740)
A2-38	6,000	5688(825)	5412(785)
A2-2	6,900	5792(840)	5206(755)
A3-9	13,320	5688(825)	5240(760)

[a] Residual stiffness at the end of low load ($n_1 = 73{,}940$ cycles).

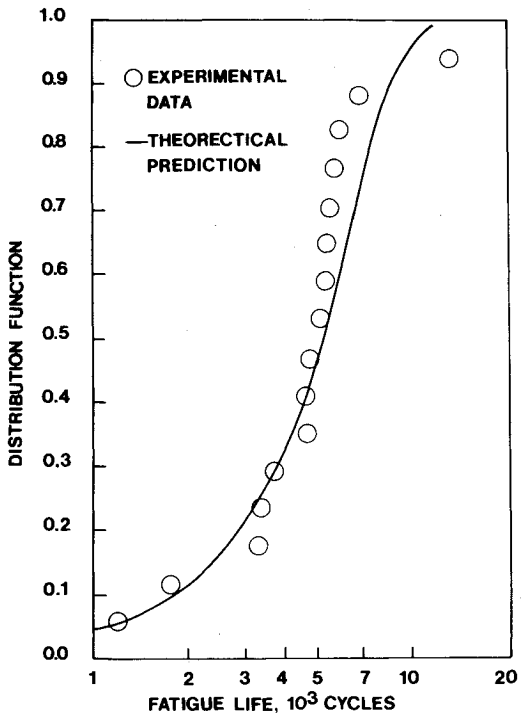

Fig. 6 Comparison between the theoretically predicted (conditional) and measured fatigue life distribution for low-high load sequence.

Table 2 Fatigue life and residual stiffness under high-low load sequence, $\sigma_{1max} = 60.7$ MPa (8.8 ksi), $\sigma_{2max} = 51.7$ MPa (7.5 ksi), $n_1 = 6030$

Specimen No.	Fatigue life under high load, cycles	Fatigue life under low load, cycles	Initial stiffness, MPa (ksi)	Residual stiffness, MPa (ksi)[a]
A1-13	3020		5516(800)	
A1-10	4800		5816(850)	
A1-54	4970		5240(760)	
A1-47	5080		5206(755)	
A2-12	2420		5447(790)	
A2-26	2480		5378(780)	
A3-46	4720		6033(875)	
A2-48		5,890	5619(815)	5171(750)
A1-5		20,090	5343(775)	4482(650)
A3-10		23,120	5516(800)	4964(720)
A2-50		30,000	5378(780)	5102(740)
A2-40		46,030	5585(810)	5102(740)
A1-43		54,760	5792(840)	4964(720)
A3-54		60,170	5929(860)	5171(750)
A1-42		66,100	5240(760)	4895(710)
A3-25		87,190	5924(860)	5164(749)
A3-39		112,660	5516(800)	5033(730)
A2-52		113,370	5240(760)	5033(730)
A2-42		122,790	5688(825)	5171(750)
A3-16		129,170	5585(810)	5033(730)
A2-22		136,500	5723(830)	5240(760)
A2-5		147,750	5861(850)	5171(750)
A3-35		182,290	5688(825)	5171(750)
A3-38		196,460	5861(850)	5447(790)
A2-11		211,890	5723(830)	5378(780)

[a] Residual stiffness at the end of high load ($n_1 = 6{,}030$ cycles).

the Miner's sum for these results is $(n_1/N_1) + (N_{12}/N_2) = (73{,}950/136{,}860) + (4810/11{,}095) = 0.9738$. It can be observed that the median value of the Miner's sum for the test results is smaller than unity as predicted theoretically, and that the correlation between the median values of Miner's sum for the theoretical prediction and that for the test results is reasonable.

Another set of 25 specimens was tested under a high-low load sequence. The specimens were subjected to a high load

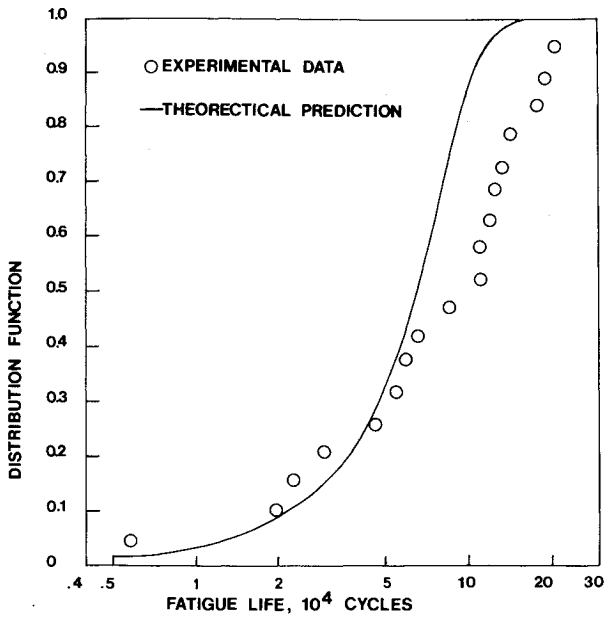

Fig. 7 Comparison between the theoretically predicted (conditional) and measured fatigue life distribution for high-low load sequence.

with a maximum stress $\sigma_{1max} = 60.7$ MPa (8.8 ksi), for 6030 cycles. Then, the specimens were further subjected to the second fatigue loading with a maximum stress $\sigma_{2max} = 51.7$ MPa (7.5 ksi) until fracture occurred. The test results are presented in Table 2.

According to the theoretical prediction given by Eq. (14), the probability that a specimen will fail under the first fatigue loading (high load) is 5%. Consequently, the average number of specimens expected to fail under the high load is $0.05 \times 25 = 1.25$ specimens.

The test results shown in Table 2 indicate seven failures, exceeding what is expected theoretically. This serious discrepancy in test results has a remarkable effect on the Miner's sum, as will be shown later. It is suspected that the discrepancy is attributed to the sampling fluctuation among panels (A1, A2, and A3), since four out of the seven failures came from panel A1. The test results for the fatigue life under the low load for those specimens which survived the high load are plotted in Fig. 7 as open circles. The distribution based upon Eq. (16) is plotted as a solid curve in Fig. 7. It can be observed from Fig. 7 that the correlation between the theoretical prediction and the test results is reasonable.

Following the same computational procedure described previously, the median value of the Miner's sum D_{50} based upon the theoretical model is computed from Eq. (22) as $D_{50} = 1.0033$. With the inclusion of the failure data, the median data point in Table 2, i.e., the 50% data point, is 54,760 cycles (the 13th data point). Therefore, the median value of the Miner's sum of the test results is $(n_1/N_1) + (N_{12}/N_2) = (6030/11{,}095) + (54{,}760/136{,}860) = 0.9436$. The main reason why the median Miner's sum is smaller than unity comes from the fact that the failure data are included. If the four failure data points from panel A1 are excluded or censored, then the median data point is 66,100 cycles and hence the median Miner's sum for the test results becomes 1.0265 which is in closer agreement with the prediction.

Finally, the elastic shear stiffness G_{12}, i.e., the shear stiffness at small stress and strain where both are related linearly, was also measured before fatigue testing and at the end of the first fatigue loading. The test results are presented in Tables 1 and 2, respectively, for both loading sequences. It is obvious from Tables 1 and 2 that the shear stiffness decays significantly under fatigue loadings,[15] although the rate of decay does exhibit considerable scatter.

Conclusions

A residual strength degradation model has been applied to predict the effect of loading sequence on the statistical fatigue behavior of advanced composites. The statistical distributions of the fatigue life and the residual strength under n stress levels of cyclic loading have been derived. An experimental test program using the graphite/epoxy $[\pm 45^\circ]_{2s}$ laminates has been carried out to generate statistically meaningful data in order to verify the validity of the theoretical approach. It is shown that the correlation between the test results and the theoretical prediction on the fatigue life distribution is reasonable.

Based upon the present model, the residual strength and its statistical distribution under n stress levels of cyclic loading (or spectrum loading) is independent of the load sequence. The statistical distribution of the fatigue life and the probability of fatigue failure do not depend on the load sequence of the previous loading history but on the magnitude of the current load cycle. As a result, both the fatigue life distribution and the fatigue reliability depend weakly on the load sequence of the entire loading history, for instance the two-stress levels loading sequence. Hence, the current model is not a linear cumulative damage model, such as the Miner's rule.

It is shown that the Miner's sum is a statistical variable. It is further proved that under two-stress levels of cyclic loading the Miner's sum is always greater than or equal to unity for the high-low sequence, and the Miner's sum is always smaller than or equal to unity for the low-high load sequence.

It has been assumed that the loss of the residual strength is irreversible and hence the residual strength decays monotonically. It does not account for the interactions between the neighboring high and low load cycles, such as the acceleration and retardation effects in the process of crack propagation in metallic materials. It is not clear at this point whether this type of interaction is important and further experimental tests are needed.

Acknowledgments

The authors would like to thank J. R. Davidson and G. L. Roderick of NASA Langley Research Center for valuable technical suggestions and discussions, and for support of this work through Grant NSG 1415.

References

[1] Salkind, M. J., "Fatigue of Composites," *Composite Materials: Testing and Design*, ASTM STP 497, pp. 143-169.

[2] Hahn, T.H., "Fatigue Behavior and Life Prediction of Composite Materials," paper presented at 5th ASTM Conference on Composite Materials, Testing and Design, New OrleaNS, La., March 20-22, 1978.

[3] Yang, J. N., "Fatigue and Residual Strength Degradation for Graphite/Epoxy Composites Under Tension-Compression Cyclic Loading," *Journal of Composite Materials*, Vol. 12, Jan. 1978, pp. 19-39.

[4] Yang, J. N. and Liu, M. D., "Residual Strength Degradation Model and Theory for Periodic Proof Tests for Graphite/Epoxy Laminates," *Journal of Composite Materials*, Vol. 11, April 1977, pp. 176-203.

[5] Yang, J. N. and Jones, D. L., "Statistical Fatigue of Graphite/Epoxy Angle-Ply Laminates in Shear," *Journal of Composite Materials*, Vol. 12, Oct. 1978, pp. 371-389.

[6] Chou, P. C., "Degradation and Sudden-Death Model of Fatigue of Graphite/Epoxy Composites," paper presented at 5th ASTM Conference on Composite Materials, Testing and Design, New Orleans, La., March 20-22, 1978.

[7] Yang, J. N. and Sun, C. T., "Effect of High Load on the Fatigue Behavior of Graphite/Epoxy Laminates," *Journal of Composite Materials*, Vol. 14, April 1980, pp. 82-94.

[8] Hashin, Z. and Rotem, A., "A Fatigue Failure Criterion for Fiber Reinforced Materials," *Glass Reinforced Epoxy Systems,* Materials Technology Series, Vol. 2, 1975, pp. 129-145.

[9] McLaughlin, P. V., Jr., Kulkarni, S. V., Huang, S. N., and Rosen, B. W., "Fatigue of Notched Fiber Composite Laminates Part I: Analytical Model," Materials Science Corp., MSC/TFR/7501, March 1975.

[10] Kulkarni, S. V., McLaughlin, P. V., Jr., and Pipes, R. B., "Fatigue of Notched Fiber Composite Laminates Part II: Analytical and Experimental Evaluation," Material Science Corp., MSC/TFR/7601, March 1976.

[11] Rankumer, R. L., and Kulkarni, S. V., "A Static/Fatigue Model for Notched Composite Laminates Including Interlaminar Effects," paper presented at 5th ASTM Conference on Composite Materials, Testing and Design, New Orleans, La., March 20-22, 1978.

[12] Broutman, L. J. and Sahu, S., "Progressive Damage of Glass Reinforced Plastics During Fatigue," *Proceedings of 24th SPI Conference*, Feb. 1969, p. 11-D.

[13] Broutman, L. J. and Sahu, S., "A New Theory to Predict Cumulative Fatigue Damage in Fiberglass Reinforced Plastics," *Composite Materials: Testing and Design (Second Conference)*, ASTM STP 497, 1972, pp. 170-188.

[14] "Composite Materials Workbook," Air Force Materials Laboratory, Technical Rept. AFML-TR-78-33, 1978.

[15] Salkin, M. J., "Early Detection of Fatigue Damage in Composite Materials," AIAA Paper 75-772, *Proceedings of the 16th AIAA/ASME/SAE Structures, Structural Dynamics, and Materials Conference*, Denver, Colo., 1975, pp. 1-8.

[16] Rosen, B. W., "A Simple Procedure for Experimental Determination of the Longitudinal Shear Modulus of Unidirectional Composites," *Journal of Composite Materials*, Vol. 6, Oct. 1972, pp. 552-554.

[17] Hahn, H. T., "A Note on Determination of the Shear Stress-Strain Response of Unidirectional Composites," *Journal of Composite Materials*, Vol. 7, July 1973, pp. 383-386.

[18] Halpin, J. C., et al., "Characterization of Composites for the Purpose of Reliability Evaluation," Air Force Materials Laboratory, Technical Rept. AFML-TR-72-289, 1972.